CLM-P682

UKAEA

Preprint

-7 FEB 1983
b

PARAMETER AND COST OPTIMISATIONS FOR A MODULAR STELLARATOR REACTOR

W. N. G. HITCHON
P. C. JOHNSON
C. J. H. WATSON

CULHAM LABORATORY
Abingdon Oxfordshire

1982

This document is intended for publication in a journal or at a conference and is made available on the understanding that extracts or references will not be published prior to publication of the original, without the consent of the authors.

Enquiries about copyright and reproduction should be addressed to the Librarian, UKAEA, Culham Laboratory, Abingdon, Oxon. OX14 3DB, England.

CLM-P 682

PARAMETER AND COST OPTIMISATIONS FOR A MODULAR STELLARATOR REACTOR

W.N.G. Hitchon, P.C. Johnson and C.J.H. Watson[†]

Culham Laboratory, Abingdon, Oxon., OX14 3DB, UK
(Euratom/UKAEA Fusion Association)

[†]Joint European Torus, Abingdon, Oxon., OX14 3EA, UK

ABSTRACT

The physical scaling and cost scaling of a modular stellarator reactor are described. It is shown that configurations based on $\ell = 2$ are best able to support adequate beta, and physical relationships are derived which enable the geometry and parameters of an $\ell = 2$ modular stellarator to be defined. A cost scaling for the components of the nuclear island is developed using Starfire (tokamak reactor study) engineering as a basis. It is shown that for minimum cost the stellarator should be of small aspect ratio. For a 4000MWth plant, as Starfire, the optimum configuration is a 15 coil, 3 field period $\ell = 2$ device with a major radius of 16m and a plasma minor radius of 2m, and with a conservative wall loading of $2MW/m^2$ and an average beta of 3.9%; the estimated cost per kilowatt (electrical) is marginally, (7%) greater than Starfire.

(Submitted for publication in Journal of Fusion Energy)

September 1982

1. INTRODUCTION

There has been recently a renewal of interest in the stellarator as a possible fusion reactor configuration, particularly as the engineering advantages of true steady state operation have been realised (even for the tokamak). This paper describes a study of the physics and costs of a fusion power plant based on the modular coil stellarator confinement system.

The use of stellarator and stellarator type devices in reactor applications is discussed in a number of publications. Unlike the tokamak, where there is a large measure of agreement on the most likely design, there is no concensus in the stellarator field on the best choice of configuration for a reactor. For modular devices, torsatron [1], stellarator [2-4] and advanced stellarator [5] concepts have been put forward. Devices with continuous helical windings such as the torsatron [6] and Heliotron [7] are also being advocated. In these publications, emphasis is placed either on the physics of the confinement system or on the engineering of the coil configurations, with little weight given to the cost economics. Costing studies have, in fact, played a major role in guiding tokamak reactor designs towards modularity, small aspect ratio and steady-state operation [8,9]. We might expect this to be true also of the stellarator [10].

In the work reported here, we have taken the modular stellarator concept and:

1. Assessed the relevant confinement physics in order to decide on the optimum flux surface geometry.
2. Developed a set of physical scaling relationships which enable the parameters of a device with a prescribed aspect ratio, wall loading etc. to be designed.
3. Developed a cost scaling for the major components of the nuclear plant, using Starfire [11] engineering as a basis. (Starfire, being a design

study for a steady-state tokamak, is particularly useful here as the engineering used can be applied with reasonable ease to the stellarator).[1]

4. Used the parameter and cost scalings to explore parameter space and optimise the stellarator for minimum cost.

It will be shown that systems based on $\ell = 2$ with a high transform per field period and a small external vertical field are best able to support the beta required for a reactor. The minimum cost device has a small plasma aspect ratio (~ 8), and for a 4000MWth plant, which is the same as Starfire, the cost, measured per unit generating capacity (1200MWe for Starfire, 1350MWe for the stellarator which does not require 150MW for current drive), is within a few percent of Starfire costs. The 'best case' design is a 15-coil 3-field period $\ell = 2$ stellarator with a major radius of 16m and a plasma minor radius of 2m. It has a modest average beta, 3.9%, and a neutron power flux to the first wall of $2MW/m^2$, which is at the lower end of the range used in tokamak reactor studies. This configuration is used as the reference case in the remainder of the paper.

2. PHYSICAL SCALING

The physical basis governing the choice of a modular coil stellarator configuration for a reactor is discussed. Relationships are derived which enable the stellarator to be modelled analytically, thus forming the basis for a cost optimization.

1. The costs we quote are all derived from those given in the Starfire report(11). Our estimate as to the cost of the stellarator reactor is, consequently, only as accurate as the Starfire costing allows. We shall not discuss the basis for the Starfire calculations in this paper, as we are primarily concerned with a comparison of stellarator and tokamak costs rather than the magnitude of those costs.

2.1 Modular coil configuration

The obvious choice of coils for a stellarator reactor is the twisted coil system proposed originally by Wobig and Rehker [2]. Typical of more recent studies are those by Anderson et al. [12] and Chu et al. [13]. This configuration can be regarded as the natural way of producing a stellarator field as it reproduces, at least qualitatively, the currents which would flow on a virtual casing enclosing the desired magnetic fields. Such coils are capable of producing nearly all of the fields necessary for a reactor, a modest vertical field system being required in addition for equilibrium near the limiting beta (see section 2.3).

The main engineering constraint of modularity is easily satisfied with this type of coil set. Wedge-shaped coils, with space allowed for the coil thickness, support structure and vacuum dewar, provide a sound basis for an engineering design. Fig. 1 shows an example of a 15 coil, 3 field-period, $\ell = 2$ set with a coil aspect ratio of $A_c \simeq 3$. Although adding in Fourier harmonics of a square wave modulation, e.g. cos $3(\ell\theta + p\phi)$ and cos $5(\ell\theta + p\phi)$, improves the quality of surfaces, we shall use the following winding law for wedge-shaped coils

$$\begin{aligned} \tilde{\phi} &= \frac{1 - R_w/R}{1 - R_w/R_o}\ \delta_1 \cos\ (\ell\theta + p\phi) \\ \tilde{\rho} &= \delta_2 \cos\ (\ell\theta + p\phi) \end{aligned} \qquad (1)$$

Here, $\tilde{\phi}$ and $\tilde{\rho}$ are the modulations in toroidal angle and radius from the minor axis normalised to the coil mean minor radius r_c), and ℓ and p are the numbers of poloidal and toroidal field periods. R is the major radius at a point on the coil, R_o is the major radius of the minor axis, and R_w is the innermost major radius which can be reached by the centre of any coil (see

Figure 2). Transform is produced principally by the modulation in ϕ. The modulation in ρ follows approximately the shape of the outer magnetic surface of the plasma, with a roughly constant separation from surface to coil. This term also serves to improve the integrity of magnetic surfaces particularly near rational values of the rotational transform ι (eg, 1/3, 2/5, 1/2 etc).

Figure 2 shows schematically the geometry of a coil, half of a module being depicted with greatly exaggerated angular width. The R-dependent factor in (1) arises for the following geometric reason: t_c is the radius of the superconducting coil and its vacuum dewar. The centre of the coil is thus constrained to lie within an envelope whose apex is at R_w. Clearly $R_w = t_c/\sin\phi_c \simeq t_c/\phi_c$, where ϕ_c is the half angle of the space allowed for one complete coil module. ϕ_c is given by $\phi_c = \pi/N_c$, where N_c is the number of coils in the main (toroidal) coil set. $\phi_1(R)$ is the maximum permissible modulation of the coil centre at R; $\phi_0 \equiv \phi_1(R_o) = \delta_1$. The scaling factor $(1-R_w/R)/(1-R_w/R_o)$ in (1) ensures that the coil reaches this maximum modulation when the trigonometric factor is unity.

It is possible to build such a coil set only if $R_w \leq R_o - a_c$, where $a_c \simeq r_c\,(1 + \delta_2)$ is the coil semi-major radius.

Factors governing the production of transform in this type of coil set are described in the next section.

2.2 Rotational transform

The profile of rotational transform in a large aspect ratio stellarator with a single ℓ component is given to lowest order by [14]

$$\iota = \frac{\ell^2(\ell-1)\ \alpha^2\,\rho^{2\ell-4}}{\bar{p}^3} \qquad (2)$$

α is a dimensionless parameter of order unity characterising the helical field strength. $\bar{p}$ is defined by the ordering assumption $p = \bar{p}\,\epsilon_c^{-2/3}$ to be

of order unity, ϵ_c being the inverse aspect ratio of the coil. The radius is normalized to the coil mean minor radius.

Thus, as is well known, $\ell = 1$ gives zero transform, $\ell = 2$ gives a flat transform profile (except where p is large when higher order terms become important) and $\ell \geq 3$ gives zero transform on axis increasing as $\rho^{2(\ell-2)}$ towards the plasma edge. Clearly as ℓ increases above 2, less and less transform is produced at lower radii, and in a reactor, where the plasma radius is of the order of half the coil radius, the higher ℓ values are unlikely to produce adequate transform in the plasma and would support therefore only a low equilibrium beta. We shall discuss this further in section 2.3.

Small aspect ratio, modular $\ell = 2$ coils do produce adequate transform to support a reasonable beta. This is contrary to the commonly held view that large aspect ratio with many field periods is necessary for high transform [15]. For example, field-line following in a modular $\ell = 2$ system with $A_c \simeq 3$, $p = 3$, $N_c = 15$ and the maximum allowed modulation within the constraints of the geometry (Figures 1 and 2) results in the vacuum surfaces shown in Figure 3. The transform is just less than $\iota_o = \frac{1}{2}$ on axis, falling to just above $\iota_r = 1/3$ at the edge. Although lowest order analytic theory predicts a constant ι, we have found that this behaviour of decreasing ι with radius is characteristic of small aspect ratio $\ell = 2$ systems, and not solely a feature of modular coils.

With a modular coil system of this type, it is difficult to obtain satisfactory fields containing large amplitudes of more than one ℓ number. Introducing a large amplitude modulation of say $\ell = 3$ into $\ell = 2$ reduces the allowable modulation on the $\ell = 2$ component, and consequently the transform on axis and beta. Therefore we choose not to consider combinations with a large amplitude of $\ell \geq 3$.

Using results from [14] (eq (11) and (16)) it is possible to show that for $\ell = 2$ the rotational transform on any magnetic surface is given by $\iota = p\delta^2$. Here, δ is the deformation of the surface, defined by the expression

$\rho \sim 1+\delta(r)\cos(2\theta + p\phi)$ which describes the first order shape of the magnetic surface. This expression for the vacuum transform is compared in Fig. 4 with values obtained by field-line following in a variety of configurations (aspect ratios, coil types, etc.). It is seen that the analytic expression is sufficiently accurate for use in reactor scaling work.

There is an upper limit to the amount of deformation which can be applied to surfaces before they begin to break open to such an extent that they are no longer suitable for plasma containment. In the remainder of this paper we take $\delta_o = 0.4$ for surfaces near the plasma axis whilst $\delta_r \simeq 0.3$ at the plasma edge (corresponding to the fall off in transform towards the edge). (The subscripts refer to values of quantities on axis and at the plasma edge respectively.) These values of δ are found, from field-line following, to be near the maximum permissible values.

In order to calculate the transform produced in any coil set, it remains to find an expression for the number of toroidal field periods p. We shall show below that p can be related to the angular width of a modular coil, which we take to be $2\phi_o$ (Fig. 2). Using results established in [14], we can apply the 'virtual casing principle' to a casing which is circular in lowest order in an inverse aspect-ratio expansion, representing the coils. The result is an expression for the currents in the casing (and hence the coils):

$$\frac{j_\phi}{j_\theta} = \frac{R_o d\phi}{r_c d\theta} = \frac{-b_\theta}{b_\phi} \tag{3}$$

The leading order terms for the normalized fields b_ϕ and b_θ are, for $\ell = 2$, [14]

$$b_\theta = -\frac{2\,\alpha\rho\,\epsilon_c^{2/3}}{\bar{p}}\sin(2\theta + p\phi)$$

$$b_\phi = 1 \tag{4}$$

Therefore, as $p = \bar{p}\ \epsilon_c^{-2/3}$ and $\rho = 1$ at the coil

$$\frac{1}{\epsilon_c}\frac{d\phi}{d\theta} = \frac{-2\alpha}{p}\ \sin\ (2\theta + p\phi) \qquad (5)$$

Thus the full angular width of the current filament in the toroidal direction is

$$2\phi_o = \frac{4\alpha\epsilon_c}{p} \qquad (6)$$

From [14] we have $\alpha = 0.5p^2\ \delta_o\epsilon_c$, and hence

$$\phi_o = \delta_o p\ \epsilon_c^2 \qquad (7)$$

Simple geometrical arguments can now be used to relate the angular width to the number of coils. We see from section 2.1 that for wedge shaped coils, $\phi_o = \pi/N_c - t_c/R_o$. Thus we have the following expression for p (which we take later to be an integer)

$$p \leq \frac{\pi/N_c - t_c/R_o}{\delta_o\epsilon_c^2} \qquad (8)$$

Given p, we can now use the relation $t_o = p\delta_o^2$ and $\delta_o = 0.4$ to estimate the transform produced in an $\ell = 2$ modular coil set. A method for determining the number of coils is discussed in section 2.4.

2.3 Beta

In previous work [14,16] we have investigated theoretically plasma equilibrium in stellarator geometries, using an inverse aspect ratio expansion to find analytic equilibria to relatively high accuracy. One result for current-free plasmas was that $\ell = 2$ stellarators are better able to support

high values of beta in equilibrium than $\ell = 3$ stellarators of the same aspect ratio and rotational transform, because of the low value of ι near the axis in $\ell = 3$. Within the range of validity of the analysis, no strict equilibrium limits on beta were found, provided that an appropriate vertical field B_v was applied to restore the outer flux surfaces. Nevertheless realistic equilibrium limits on peak beta (set by requiring that the outer flux surfaces should not be too distorted) calculated for quartic pressure profiles, representative of an α-heated reactor plasma, are $\beta_o \leq 2\iota_o^2\epsilon_p$ for $\ell = 2$ and $\beta_o \leq \frac{1}{2}\iota_r^2\epsilon_p$ for $\ell = 3$. Figure 5 illustrates a computed equilibrium for $\ell = 2$ with a transform of $\iota_o = 0.48$ and a plasma inverse aspect ratio of $\epsilon_p = 1/8$. The peak beta is $\beta_o = 5.8\%$ and the applied vertical field is $B_v = 0.04\ B_o$ (B_o is the strength of the main field on the minor axis).

Calculations presented by Lortz and Nuhrenberg [17] based primarily on equilibrium considerations show smaller values of limiting beta. Reasons why their calculations lead to an overpessimistic beta limit were given in [14]; the are:

1. They impose a circular magnetic axis, which implies a substantial applied vertical field, exactly compensating the axis shift. This will have a detrimental effect on the magnetic surfaces. If the axis is allowed to shift from its vacuum position, it also spirals: it is allowed to do so in our calculation [14].

2. The Mercier expansion which they employ is not of sufficient accuracy near the separatrix.

MHD instabilities can in principle limit the maximum beta below the equilibrium limit. In a current-free stellarator, the most important modes are those driven by the plasma pressure. We distinguish two varieties of these, ballooning modes and modes localised around a rational surface, and show that both should lead to critical beta values comparable with or greater than the equilibrium limit described above.

An approximate stability criterion for ballooning modes was given in [18] as $\beta_c \leq rR_c/L^2$, where r is the pressure scale length, R_c the mean radius of curvature and L the connection length between regions of favourable curvature. For a tokamak, $r \simeq r_p$ (plasma radius), $R_c \simeq R_o$ and $L \simeq qR_o$, and the critical beta is $\beta_c \simeq \epsilon_p/q^2 = \iota^2\epsilon_p$. In a stellarator with a large helical modulation, the connection length is of the order of a field period and the field line curvature is dominated by the helical field, as opposed to toroidicity, and the net result is a critical beta substantially greater than that for a tokamak [19]. When the helical modulation is relatively small, the toroidal curvature dominates except in regions close to the top and bottom of the minor cross-section where the helical field takes over. In the particular case of an $\ell = 2$, $p = 3$ stellarator with $A_p = 1/\epsilon_p = 8$ and $\iota_o = 0.48$ the helical field provides favourable curvature within about 30° in poloidal angle from the top and bottom of the minor cross-section. The connection length is then $L \simeq \frac{2}{3} qR_o$ and consequently the ballooning stable beta is approximately $\beta_c \simeq 2.2\ \epsilon_p/q^2$, which is of the same order as the limiting peak beta from equilibrium, and so ballooning stability is not expected to set a lower limit on beta than that imposed by equilibrium considerations.

Localized modes which grow in the vicinity of the mode rational surface have been shown theoretically [20] to be stabilized by shear and by the presence of a magnetic well. In most stellarators there is a large shear in the field, and these modes should then be stable according to ideal MHD theory. Finite resistivity virtually removes the effect of shear in the stabilization of these instabilities, as shown in [14] where the criteria given in [21, 22] are evaluated for stellarator geometries. It was found that for low beta $\ell = 2$ equilibria, stability was predicted if $p\iota < 11/2$. This inequality is close to the condition for the formation of a magnetic well. It is satisfied in small aspect ratio $\ell = 2$ stellarators where p is not too large (in section 2.2 it was shown that $\iota = p\delta^2$; we take $\delta = 0.4$ and thus p should be less than 5).

The conclusions arising from this section are:

1. $\ell = 2$ is a better choice on equilibrium grounds than $\ell \geq 3$.
2. Sensible equilibria for $\ell = 2$ are obtained for $\beta_o \lesssim 2\iota_o^2\epsilon_p$.
3. Pressure-driven MHD instabilities should not impose a lower beta limit in a small aspect ratio $\ell = 2$ stellarator with $p \leq 5$.

2.4 Separatrix formation

The separatrix in a stellarator with ℓ-windings is formed when lines of force orbit poloidally around the windings preventing the formation of closed surfaces. This is not the case in an $\ell = 2$ stellarator with modular coils. Here the open field lines circulate toroidally around the coils, as in any discrete-coil solenoid. The helical symmetry of the ℓ-winding separatrix is lost in the modular system.

In the modular coil set, the mean coil spacing is $2\pi R_o/N_c$. The distance between the separatrix, radius r_{SX}, and the coil, radius r_c, is found in the absence of field errors to be a maximum of half the mean coil spacing. This is shown in Fig. 6, where field-line following results on $(r_c - r_{SX})/R_o$ are plotted against π/N_c, for a variety of coil systems. We can use this observation to determine the minimum number of coils. Obviously the separatrix should occur at, or further out than the first wall, mean radius r_F. Thus we hav

$$r_{SX} \geq \left(r_c - \frac{\pi R_o}{N_c}\right) \geq r_F \tag{9}$$

and hence

$$N_c \geq \frac{\pi R_o}{(r_c - r_F)} \tag{10}$$

2.5 Coil conductor size

The finite size of the conductors, which we take here for simplicity to be circular, radius S_c, imposes a major constraint on the geometry of the main

coil set. In effect it reduces the transform available at a given major radius, as the space occupied by the coils is unavailable for extra coils or greater coil modulation. Obviously in a detailed design for an actual device, the size and shape of the coil conductors would be the subject of an extensive study, beyond the scope of the present work. We shall derive here a simple formula to calculate the coil conductor radius S_c which is adequate for the scaling work presented later.

The magnetic field strength at the surface of a conductor is generally taken to be limited to $B_c \simeq 10\text{-}11$ T by the strength of materials. Where the coils are spaced apart, as they are in a modular stellarator (Fig. 1) the main contribution to the surface field comes from the self-field due to the conductor current I_c ; $B_c = \mu_o I_c / 2\pi S_c$. The current in a coil required to provide a main field B_o at R_o is $I_c = 2\pi R_o B_o / N_c \mu_o$, and thus we have a simple relation for S_c:

$$S_c = R_o \frac{B_o}{B_c N_c} \qquad (11)$$

We have neglected here the increase in the field on the inboard coil limbs due to the shared flux. We shall make some allowance for this by taking a pragmatic value for B_c in (11) of 10 Tesla. In fact (11) leads to conductor sizes which are typical of tokamak reactor designs (i.e. in the range $2S_c \simeq 1\text{-}1.5$m).

2.6 Fusion power output

Once the geometry and the beta of a fusion device are fixed, the requirement to produce a given output power determines the main field at which the device must operate. The fusion power density appropriate to a reactor plasma can be expressed as [23]:

$$P_v = 1.44\ \beta^{*2}\ B_o^{\,4}\ \text{MW.m}^{-3} \qquad (12)$$

where β^* is the root-mean-square toroidal beta.

This relation is evaluated for the maximum reaction rate, at an ion temperature T_i = 13 keV, and takes 20 MeV per reaction, thereby including a contribution from breeding in the blanket as well as plasma fusion products. We shall be interested later in the neutron power produced in the plasma, and this is given by:

$$P_n = f_1 f_2 f_3 P_v = 0.4\ \beta_o^2 B_o^4 \quad MW.m^{-3} \tag{13}$$

where f_1 = 8/15 converts β^{*2} to β_o^2 for a quartic pressure profile (as used in the equilibrium calculations, section 2.3), $f_2 = 0.86^2$ allows for depletion of D-T by 14% helium pressure (as Starfire) and f_3 = 0.7 represents the contribution from 14.1 MeV neutrons. We shall use this expression rather than one derived from Starfire parameters, as the stellarator can operate at T_i = 13 keV whereas Starfire needs a higher T_i (hence a lower P_n) to maximise the efficiency of the lower hybrid current drive.

The total thermal output power is now

$$P_{TH} = \eta_{TH} P_n V \tag{14}$$

where η_{TH} = 1.43 is the breeding ratio (including fusion α-particles) and V is the volume of reacting plasma. Also,

$$P_{TH} = \eta_{TH} P_w A_w \tag{15}$$

where P_w is the mean neutron power loading on the first wall, and A_w is the area of the first wall. It is well known from tokamak reactor studies that the cost of the installed capacity decreases as P_w is raised, and the Starfire group chose to operate at P_w = 3.6 MW/m^2, which is at the upper limit for known materials. However, there is an advantage to be gained in replacement lifetime by operating at lower P_w. We shall discuss these points further for

modular stellarators in section 4.

2.7 Transport and Heating

Although there is recent experimental evidence that confinement in net-current free stellarators is neoclassical [24], in this work we take the empirical INTOR scaling, $\tau_E = 5.10^{-21} \bar{n}\, r_p^2$, to be consistent with the majority of reactor studies. τ_E is the energy confinement time, $\bar{n}$ the mean electron density and r_p the mean plasma radius. It is simple to estimate from this scaling the additional heating power required for ignition,

$$P_H = \tfrac{1}{2}.\frac{3\bar{n}e\bar{T}}{\tau_E}.V \qquad \text{(Watts)} \qquad (16)$$

where V is the volume and the factor $\frac{1}{2}$ allows for the contribution of α-heating as ignition is approached. $\bar{T}$ is the mean temperature at ignition (in eV). Substituting for τ_E, we have $P_H = 10^3 \bar{T} R_o$, and with $\bar{T} = 10^4$eV, we find $P_H = 10R_o$ (MW). We shall use this expression in estimating the cost of heating.

At ignition, the α-power is greater than or equal to the transport losses

$$\frac{(0.86\bar{n})^2}{4} \langle\sigma v\rangle e Q_\alpha \geq \frac{3\bar{n}e\bar{T}}{\tau_E} \qquad (17)$$

Q_α is the α-particle energy, $Q_\alpha = 3.5$ MeV, and $\langle\sigma v\rangle$ is the reaction rate, given approximately by $\langle\sigma v\rangle \simeq 1.2\ 10^{-30}\ T^2$ $(m^3 s^{-1})$ for T in the range 8-20 keV. The factor 0.86 with $\bar{n}$ on the left-hand side of (17) allows again for a 14% dilution of D-T by helium ions. We then have, on substituting for τ_E, a criterion on $\bar{n}r$ for ignition

$$\bar{n}r \geq \frac{2.8\ 10^{22}}{\bar{T}^{\frac{1}{2}}}\ m^{-2} \qquad (18)$$

which with $\bar{T} = 10^4$ eV is $\bar{n}r_p \geq 2.8\ 10^{20}\ m^{-2}$.

We can use this, with expressions from section 2.6, to estimate the minimum r_p for ignition. Combining (14) and (15) we have $P_n V = P_w A_w$. For a circular cross-section we have $V/A_w = r/2$ (neglecting any boundary layer). Also we have, from (13), $P_n = 0.4\ \beta_o^2 B_o^4$ (MW/m^3), which with $\beta_o = \frac{3}{2}\bar{\beta}$ (quartic pressure profile) and $\bar{\beta} = 2\bar{n}e\bar{T}/(B_o^2/2\mu_o)$ gives

$$\bar{n}\ \bar{T}\ r^{\frac{1}{2}} = 1.85\ 10^{24}\ P_w^{\frac{1}{2}} \qquad (19)$$

where P_w is in MW/m^2. Combining (18) and (19), and taking $\bar{T} = 10^4$ eV, we then find:

$$r \geq \frac{2.3}{P_w} \qquad (20)$$

Taking typical wall loadings of 2 - 3.6 MW/m^2 leads to minimum r in the range 0.65 - 1.2 m, which, as we shall see later, is quite easy to achieve in a modular stellarator.

2.8 Boundary control

It is often said that the stellarator possesses a natural divertor, referring to the ridge with helical symmetry which occurs at the separatrix in stellarators with ℓ-windings; field lines outside the separatrix orbit the ℓ-windings forming the divertor. In some modular systems, localized divertor regions can be found which follow the dominant pitch-angle of the winding system [25], although we have not found such a pattern in the $\ell = 2$ coil sets we have analysed. Both of these divertor configurations rely on the vacuum-field separatrix being inside the first wall, which may be undesirable as the outer flux surfaces are lost first when beta increases, leading to a reduction in the useful plasma volume. The presence of a vacuum-field separatrix is not necessarily an important feature of the $\ell = 2$ modular systems discussed in this paper.

A more promising approach to boundary plasma control in such coil sets is the combination of a 'resonant helical divertor', described for a tokamak by Karger and Lackner [26], with a pumped limiter. The principle behind the resonant helical divertor for a tokamak is the creation of a resonant magnetic island in the boundary plasma by the addition of a helical winding. Transport across this island structure is enhanced, so that a pumped limiter inserted into the island would be subject to more uniform heat and particle loading mainly on the back surface facing the pump. The coil set in Fig. 1 produces $q \simeq 3$ at the plasma boundary. The design of a modular coil system could be readily optimized to produce an island of the right magnitude to form a useful divertor, without seriously affecting the transform on axis.

2.9 Forces

The full coil set of a modular stellarator (as envisaged in this work) consists of a set of main field coils, such as those depicted in Fig. 1, and a pair of vertical field coils sitting outside the main coil set at the top and bottom of the machine (see Fig. 8). These latter coils are required for equilibrium at the ignition beta. We have made estimates of the main forces in such a system in order to see whether they are within sensible engineering limits.

Taking the parameters of an optimum design (section 4; $N_c = 15$, $p = 3$, $B_o = 6.6T$, $R_o = 15.8m$, $r_c = 5.5m$, $B_v = 0.26T$), the main forces and their magnitudes are:

1. Coil self-expansion force, acting in the minor-radial direction, of $F_1 \simeq 2\pi R_o B_o^2/\mu_o N_c = 2.25\ 10^8$ N m $^{-1}$ per unit length.
2. Coil centering force, acting towards the major axis, of approximately (for a circular coil) $F_2 \simeq F_1 . \pi r_c / A_c = 1.4\ 10^9$ N per coil ($A_c = R_o/r_c$).

3. Coil toppling force, due to the interaction with B_v, resulting in a turning moment of $T_3 = 4r_c^2 B_v . 2\pi R_o B_o / \mu_o N_c = 1.1\ 10^9$ Nm, or a force $F_3 \simeq 1.10^8$ N acting on the top and bottom of a coil.

4. Coil-to-coil attractive force, arising out of the interaction between neighbouring coils where their toroidal modulation brings the conductors relatively close together. Approximating the adjacent sections as parallel straight conductors, we find a force per unit length $F_4 \simeq \mu_o (2\pi R_o B_o / \mu_o N_c)^2 / 2\pi d \simeq 2.4\ 10^8$ N m^{-1} where we have taken the separation $d \simeq 1$m.

The forces F_1, F_2 and F_3 are present in tokamaks, but the magnitude of the toppling force F_3 is reduced because of the smaller vertical field. The coil-to-coil attractive force F_4 is of a similar magnitude to F_3, and both should readily be supported by a conductor/casing design which will withstand F_1 and F_2. We may note also that the attraction between neighbouring coils gives rise to a force acting poloidally, but the net force is small when the contributions from both near neighbours are taken into account.

The potential of the stellarator for true steady-state operation reduces the number of cycles through which the coils are taken in the life of the reactor as compared to a pulsed device. Thus materials can be used much closer to their yield limits without the risk of fracture due to cyclic stresses

3. COST SCALING

In this section the geometry of a stellarator reactor based on Starfire design concepts [11] is described first. Then, the method of calculating reactor parameters, using results from section 2, is summarized. The costing scheme for the stellarator power station is then described. This is based on Starfire cost estimates (in \$1980), and as the plant thermal output is kept the same as Starfire (4000 MW), cost scalings only of the major components

of the stellarator reactor and its containment building are required, with the balance of plant (thermal, electrical, services, etc.) remaining unchanged. Starfire parameters and costs are outlined in Tables 1 and 2.

3.1 Reactor geometry

A schematic representation of the poloidal cross-section through a modular stellarator based on Starfire design concepts [11] is depicted in Fig. 7. The shape of the major components is approximated by ellipses, concentric with the minor axis: this provides a simple means for calculating volumes etc. which we shall need for the costing scheme. (We use the terminology, with appropriate suffixes: a - semi-major axis; b - semi-minor axis; r - mean radius (a+b)/2; e - elongation a/b)

The outer flux surface of the reacting plasma is represented by an ellipse with an elongation of $e_p = 1.85$. This corresponds approximately to the surface given by field-line following for a modular $\ell = 2$ coil set, Fig. 3. The plasma is surrounded by:

1. Boundary layer for exhaust limiter, 0.2m in extent,
2. First wall and blanket, 0.6m thick,
3. A vacuum space for torus and exhaust pumping, 0.7m wide,
4. Neutron shield, 1.1m thick,
5. Main coil dewar, total width 0.2m, enclosing
6. Main coil, with conductor radius s_c found by parameter optimization (section 3.2).

Openings in the blanket, for the limiter, and in the shield, for the pumping ducts, are not shown.

A section through the stellarator in its reactor building is shown in Fig. 8. The positions of the equilibrium coils are indicated. The dimensions of the reactor building allow for the complete removal of one coil module for maintenance.

The methods of calculating reactor parameters and component costs based on this representation of the geometry are described in the next two sections.

3.2 Reactor parameters

The parameters of an $\ell = 2$ modular stellarator reactor are calculated as follows: at a given P_w, A_w is determined from $P_w A_w = P_{TH}/\eta_{TH} = 2810$ MW, (15) A value is chosen for r_p, and hence a_p and b_p for $e_p = 1.86$, and then R_o is calculated using $A_w = 4\pi^2 R_o \{(a_F^2 + b_F^2)/2\}^{\frac{1}{2}}$, where $a_F = a_p + 0.2$ and $b_F = b_p + 0.2$ allowing for the 0.2m boundary region between the plasma edge and the first wall. The mean coil radius is found from $r_C = r_p + 2.8 + S_c$, assuming a value for S_c; this takes into account all of the space used between the plasma and coil conductor. N_c is given by the constraint on the position of the separatrix, $N_c \geq \pi R_o/(r_C - r_F)$, (10). p is given by (8), $p \leq (\pi/N_c - t_c/R_o)/\delta_o \epsilon_c^2$, where $t_c = S_c + 0.2$, $\delta_o = 0.4$ and $\epsilon_c = r_C/R_o$. We can then calculate beta, as $t_o = p\delta_o^2$ and $\beta_o = 2t_o^2 \epsilon_p$. B_o is found using (13), $P_{TH}/\eta_{TH} = P_n.V = 0.4\ \beta_o^2 B_o^4 V$, where $V = 2\pi^2 R_o a_p b_p$ is the plasma volume. B_c is then estimated from (11), $B_c = B_o R_o/S_c N_c$, and the above process repeated varying S_c (at fixed P_w, r_p) until $B_c = 10T$ (or S_c is a minimum radius of 0.5m). The reactor parameters for this wall loading and minor radius are then defined.

3.3 Component costs

We describe the cost scaling of each of the major components of the reactor in turn, using Starfire engineering and costs as a basis.

3.3.1 First wall and blanket

The Starfire first-wall and blanket design consists of a beryllium-coated PCA stainless steel first wall, Be or Zr_5Pb_3 multiplier, $LiAlO_2$ (60% enriched) breeder and a graphite reflector. The structure is PCA stainless steel, and pressurized water is the cooling medium. The total thickness of the first-wall/ blanket sandwich is 0.6m ('outboard' side, the 'inboard' first-wall/blanket beir

somewhat thinner due to the omission of the graphite reflector and some breeder material). Maintaining this first-wall/blanket thickness around the stellarator plasma, we take the cost C_{FWB} to be proportional to the volume, $V_F = 0.6.4\pi^2 R_o \{(a_F'^2 + b_F'^2)/2\}^{\frac{1}{2}}$. $a_F' = a_p + 0.5$ and $b_F' = b_p + 0.5$ are the average semi-major and minor axes of the first-wall/blanket. The constant of proportionality, derived from Starfire data is 0.17 \$M/m^3 (Zr_5Pb_3 breeder option):

$$C_{FWB} = 0.17\ V_F \qquad (\$M) \qquad (21)$$

3.3.2 Neutron shield

In the Starfire design, the inner surface of the shield acts as a vacuum wall for the torus. A plenum, 0.7m wide, is provided between the blanket and shield on the 'outboard' side to give a large pumping conductance for the exhaust from the pumped limiters. As space is available on the inboard side of a stellarator, we can extend this vacuum region so that it surrounds the entire blanket (Fig. 7).

The geometry of a stellarator also allows for a uniform thickness of shield surrounding the plasma. We can base the cost estimates for the stellarator therefore on the cheaper outboard shield design for Starfire. This is constructed of layers of high-flux shield, 5% Ti6Al4V + 65% TiH_2 + 15% B_4C + 15% H_2O, medium-flux shield, 70% Fe-1422 + 15% B_4C + 15% H_2O and low-flux shield, 100% Fe-1422. The total thickness is 1.1m. Again we take the cost C_5 to be proportional to the volume, $V_s = 1.1.4\pi^2 R_o \{(a_s^2 + b_s^2)/2\}^{\frac{1}{2}}$, maintaining the 1.1m thickness and with $a_s = a_p + 2.05$ and $b_s = b_p + 2.05$. The cost per unit volume, estimated for the Starfire outer shield is $4.74\ 10^{-2}$ \$M/m^3. To this cost we add a fixed amount, \$76.8M, for the pumping duct shielding as in Starfire:

$$C_s = 76.8 + 4.74\ 10^{-2}\ V_s \qquad (\$M) \qquad (22)$$

3.3.3 Main coil set

The design of the Starfire toroidal coils uses NbTi and Nb_3Sn superconductor materials in a copper stabilizer with epoxy-fibreglass laminate insulation material. Each coil is cooled in a liquid-helium bath: we have allowed for a 0.2m liquid helium dewar around the modular stellarator coil in the present conceptual design. We take the cost of a coil set C_{TF} to scale with the current necessary to generate the main field B_o on axis, $I_c = 2\pi R_o B_o/\mu_o$, and the length of each coil, $L_c \simeq 2\pi\{(a_c^2 + b_c^2)/2\}^{\frac{1}{2}}$ (neglecting the ϕ modulation). The proportionality constant, derived for the Starfire coils, is equal to $1.55.10^{-2}$ \$M/MA-m, and thus

$$C_{TF} = 1.55\ 10^{-2}\ I_c L_c \qquad (\$M) \qquad (23)$$

3.3.4 Equilibrium coil set

The modest vertical field required to restore the outer flux surfaces in the stellarator can be generated by two simple coils placed outside the main coil set, as shown in Fig. 8. The major radius of the coil conductor axis R_E is 1.5m outside the envelope of the main coil set, $R_E = R_o + a_c + t_c + 1$ where $t_c = S_c + 0.2$. The vertical field at a typical R_o from two such coils has been computed to be $B_v = 0.83.\ \mu_o I_E/2R_E$, where $\mu_o I_E/2R_E$ is the field at the centre of a single coil. For equilibrium we require $B_v \simeq 0.04\ B_o$ (section 2.3) and thus $I_E = 2R_E.\ 0.04\ B_o/0.83\ \mu_o$. Again we take the cost C_{EF} proportional to $I_E L_E$, where $L_E = 2\pi R_E$, and with a constant of $1.32\ 10^{-2}$ \$M/MA-m derived from the 8 EF coils in the Starfire design:

$$C_{EF} = 1.32\ 10^{-2}\ I_E.2\pi R_E \qquad (\$M) \qquad (24)$$

The Starfire design also calls for a set of correction field coils with a faster response than the main equilibrium coils. The cost of these coils is

modest, and we have retained them for the stellarator without scaling.

$$C_{CF} = 4 \qquad (\$M) \qquad (25)$$

The ohmic coils in the Starfire design are not required for the stellarator.

3.3.5 Plasma heating

Lower-hybrid radio-frequency heating was chosen for heating to ignition and current drive on Starfire. To be consistent with the Starfire study, we retain this heating method, and its costs, for the stellarator. The power required to heat the stellarator to ignition on a time-scale much longer than the energy confinement time was estimated in section 2.7 to be $P_H = 10R_o$ (MW), which is consistent with the Starfire heating power of 90.4 MW. The cost per unit power used in the Starfire study (not including power supplies) is 0.372 \$/W, and hence the cost of heating the stellarator to ignition is

$$C_H = 0.372\ P_H \qquad (\$M) \qquad (26)$$

3.3.6 Power supplies

In order to calculate the cost of power supplies, switching and energy storage appropriate to a stellarator reactor, we take each of the component systems in turn and scale costs from Starfire figures:

Main (TF) coils - scale the cost with $I_c L_c$ as (23)

$$C_{TFPS} = 3.75\ 10^{-5}\ I_c L_c \qquad (\$M) \qquad (27)$$

Equilibrium coils - also scale as $I_E L_E$ (24)

$$C_{EFPS} = 1.03\ 10^{-2}\ I_E . 2\pi R_E \qquad (\$M) \qquad (28)$$

Correction field coils - retain unchanged

$$C_{CFPS} = 9.3 \qquad (\$M) \qquad (29)$$

Ohmic coils - not required

ECRH start-up - retain unchanged

$$C_{ECRH} = 3 \quad (\$M) \tag{30}$$

Lower hybrid heating - scale with P_H (26)

$$C_{HPS} = 0.126 \cdot P_H \quad (\$M) \tag{31}$$

3.3.7 Reactor buildings

The reactor building for the Starfire device consists of two parts, the reactor hall (50 x 50 x 42.5m high) and a process module room (70 x 50 x 42.5m high) where large torus components are prepared or rebuilt. All contaminated or potentially contaminated systems are located within this building. In order to find the costs of the stellarator reactor building, we consider that a process module room of similar size would be required, at a pro-rata cost of \$91.48M, and that we can scale the cost of the reactor hall by volume, V_{BLD}, assuming it to be a box as in the Starfire design. The width of the reactor hall must be enough to accommodate a complete main coil sector removed from the reactor, Fig. 8. We allow a further 3m space around the withdrawn module, and thus the distance from the machine axis to the face of the wall must be $R_o + 3(a_c + t_c) + 3$. To calculate the height, we allow a headroom of 30m above the coil envelope, giving a height of $2(a_c + t_c) + 30$. The cost per unit volume of the Starfire reactor hall is $6.17\ 10^{-4}$ $\$M/m^3$, and thus the total cost of the stellarator reactor building is

$$C_{BLD} = 91.48 + 6.17\ 10^{-4}\ V_{BLD} \quad (\$M) \tag{32}$$

3.4 Cost summary

The cost of the remainder of the stellarator reactor power station plant, that is apart from the items discussed above, is taken to be identical to

Starfire. This should be a good approximation as we have chosen to cost a station with the same thermal output power, P_{TH} = 4000 MW. The total cost of this 'balance of plant' is $1029.33M, to which we add the scaled costs of the separated items in order to derive the total direct cost.

The cost accounting scheme used by Starfire then adds 23% to the total direct cost for the provision of construction facilities, equipment and services (10%), engineering and construction management services (8%) and other costs (5%). To this new subtotal is added a further 13% for inflation during construction (keeping to the 1980 constant dollar scheme), giving the total capital cost.

The best comparator of the capital cost of generating plant is the cost per unit of installed capacity, C_u. This is obtained for the stellarator power station by dividing the total capital cost by the electrical power output, which is 1350 MW. This is 150 MW higher than Starfire, where this amount of power is recirculated to supply the lower hybrid current drive (not required on a stellarator).

4. RESULTS AND DISCUSSION

The results of calculations of stellarator reactor parameters and costs are presented. It is shown that the geometry and cost scalings lead to a design with a relatively small aspect ratio and modest wall loading, and that such a design, producing slightly more electrical power than Starfire for the same thermal output, is not significantly different in the cost per unit installed capacity from Starfire. The significant reductions in cost per kilowatt which occur when less conservative values of beta and wall loading are allowed, are discussed at the end of the section.

4.1 Geometry and parameters

The effect of P_w, and hence A_w, on the parameters of an $\ell = 2$ modular stellarator reactor is evident from Figs 9 and 10. Fig. 9 shows, on contours of constant wall loading, the loci of parameters r_p and R_o for devices with minimum R_o (which is also a guide to minimum cost) at given numbers of field periods. The weak variation of R_o with P_w occurs because a minimum circumference is required to fit in a sufficient number of finite-diameter coils with adequate modulation to produce the required transform. B_o, and hence S_c, increase with P_w for these minimum R_o devices (Fig. 10a) exacerbating the space problem to the point where it is no longer possible to construct a device if we adhere to the 10 Tesla restriction on B_c, eg, $p = 3, 4, 5$ at $P_w = 3.5 MW/m^2$ in Fig. 9.

The variation of N_c, p, β_o, B_o, S_c (and the cost per unit installed capacity) with plasma aspect ratio A_p is shown in Fig. 11 for $P_w = 2 MW/m^2$, and again choosing devices with minimum R_o at a given p. The parameter optimisation scheme we have used corresponds to choosing the minimum number of coils consistent with the separatrix being at or outside the first wall, and then allowing the coils to have sufficient modulation to produce the rotational transform (fixed at 0.16 per field period), without overlapping. It is evident from Fig. 11 that as A_p is reduced, fewer coils can be fitted in. This reduces the number of field periods and hence the axial beta, and consequently the main field must increase (to maintain constant power output) requiring larger coil conductors to maintain $B_c \lesssim 10T$.

It should be noted here that all of the configurations identified in Figs. 9-11 have a minor radius in excess of that required to satisfy the ignition criterion (20) based on INTOR scaling of τ_E.

We conclude here that there is no obvious choice of optimum configuration which can be made purely on the basis of reactor parameters.

4.2 Costs

The calculated cost per unit installed capacity C_u is shown in Fig. 10b as a function of wall loading P_w (for p = 3) and Fig. 11f as a function of plasma aspect ratio A_p (for $P_w = 2MW/m^2$). There is a steep rise in C_u below $P_w = 2MW/m^2$ (Fig. 10b) mainly through increases in the volumes of blanket, shield and buildings. Figure 11f shows that C_u decreases steadily as A_p is reduced, with a broad plateau at $A_p \lesssim 10$. The variation in component costs with A_p is shown in Figure 12; it is clear that the trend in C_u is a consequence of the addition of a number of small effects rather than a large variation in one major component. The major costs are in the reactor buildings and the main coil set, with the shield and first-wall/blanket slightly below. C_{TF} increases at small aspect ratio because of the increase in B_o (Figure 11d).

Although the costs of the components of the nuclear island appear substantially higher for a stellarator than for the Starfire tokamak (which has the lowest costs of any tokamak reactor design, and is also steady-state), the stellarator does in fact produce ≈ 11% more electrical power for the same thermal power and hence the overall cost per unit power can be reduced to a level very close to Starfire ($2000/kW at 1980 prices).

It is clear then that the 'minimum cost' stellarator reactor will have a modest plasma aspect ratio $\lesssim 10$, a small number of field periods (2-4) and a reasonable wall loading (2-3MW/m^2). If we set a further constraint, that N_c must be an integral multiple of p, the choice would appear then to be between (10, 2, 2.5), (12, 2, 2), (12, 3, 3) and (15, 3, 2) (where the parameters are N_c, p, P_w). The values of main field B_o and

cost/kW C_u for these devices are (8.2, 2041), (7.8, 2162), (8.5, 2060) and (6.6, 2154).

We have chosen here to present detailed lists of parameters and costs (Tables 1 and 2) for the 15 coil 3 field period device, which offers the most conservative values of B_o and P_w. The data for Starfire are also given in Tables 1 and 2. The average plasma radius of the stellarator is $r_p \simeq 2$m, slightly below Starfire, and the major radius is $R_o \simeq 16$m, giving $A_p \simeq 8$. The coil aspect ratio is $A_c \simeq 2.9$. The parameters call for a modest peak beta, $\beta_o = 5.8\%$ (viz, $\bar{\beta} = 3.9\%$) which is well below the Starfire beta ($\beta_o = 19.4\%$, $\bar{\beta} = 6.7\%$, where it should be noted that $\bar{\beta} \simeq 6\ \epsilon_p/q^2$). Figure 13 shows the effect of increasing the equilibrium beta in the stellarator (with p = 3) from the value used in the main study, $\beta_o = 2\iota_o^2\ \epsilon_p$ up to $\beta_o = 4\iota_o^2\ \epsilon_p$. The cost per kilowatt at this higher beta is now some 5% below Starfire at $P_w = 2.5\text{MW/m}^2$. However we do not wish to claim that the stellarator would provide such a high beta.

Similar reductions in the cost per kilowatt could be achieved by increasing the size of the device to produce a higher output: the thermal power of 4000MW was chosen for the present study to be compatible with Starfire. This applies also to the tokamak, and gives no particular advantage to the stellarator.

5. COMPARISON WITH OTHER STELLARATOR REACTOR STUDIES

There are two published studies of modular-coil stellarator reactor designs with which we can compare the 'best case' described above [Tables 1 and 2]. These are the Wisconsin study UWTOR-M [3], which is $\ell = 3$, and the Los Alamos study MSR [4], which like our device is $\ell = 2$. Costs are not discussed in the Wisconsin work.

Analytic theory of equilibria in stellarators [14, 16] is used in the present work as a basis for choosing $\ell = 2$ rather than $\ell = 3$ (section 2.3). This theory suggests that the average beta assumed for UWTOR-M, $\bar{\beta} = 0.06$, would lead to a very large axis shift, and that a value $\bar{\beta} \simeq \frac{1}{2}\beta_o \simeq \frac{1}{4}\iota^2/A_p = 0.022$ would be more appropriate ($\iota = 1.125$ and $A_p = 14$ in UWTOR-M). This would appear to pose a serious problem for an $\ell = 3$ design. In order to achieve the high value of rotational transform at the separatrix in UWTOR-M, the Wisconsin group have used a large number of toroidal field periods ($p = 6$). This inevitably leads to a large aspect ratio ($A_c \simeq 5$). The main result of the cost analysis in the present work is that for minimum cost a stellarator (like a tokamak) must have a small aspect ratio. UWTOR-M would appear therefore not optimized in terms of cost.

The Los Alamos modular stellarator reactor, MSR, is $\ell = 2$. An expression for the maximum beta is used, $\bar{\beta} = \iota^2/A_p$, which is similar to the one used here, $\bar{\beta} = 4/3\ \iota_o^2/A_p$. The difference is due, in large part, to the use of an external vertical field in the present work to restore the outer flux surfaces. This leads to a better utilization of magnetic volume from low to high beta, and we believe it to be an important feature of the modular stellarator concept. The main difference between MSR and the present work is to be found in the method of producing transform. MSR relies on a large number of field

periods, $p \geq 6$, which (like UWTOR-M) leads to a larger aspect ratio than is necessary on grounds of cost. In fact, the plasma aspect ratio in MSR is modest, $A_p = 11$; this is a consequence of the use of a rather low neutron wall loading $P_w = 1.3$ MW/m^2, which allows the use of a larger minor radius. (eg see Figure 9). The MSR group experience some difficulty in producing the assumed transform, $\iota = 0.66$, by field-line following which gives $\iota = 0.15$. The higher value is the transform calculated for a conventional helical coil stellarator with the same A_c and p, and with the separatrix close to the coils. They point out however that a conventional stellarator is not a good analogue of a modular coil system, and that a better analogue [13] which takes into account the 'anti-helical' winding as well as the 'helical' winding gives better agreement with field-line following. In fact we know that the separatrix is not helical in modular $\ell = 2$ devices, but arises out of the finite separation between the coils (section 2.4); we use this feature in the present work to determine the number of coils. For MSR parameters, $P_{th} = 4800$ MW, $P_w = 1.3$ MW/m^2, $p = 6$, $\iota = 0.66$, we have calculated the size and cost of an $\ell = 2$ reactor system using the model described in this paper. The result, $R_o = 25.4$ m, $r_p = 2.33$m, $A_p = 10.9$, $A_c = 4.5$, $N_c = 24$, $\bar{\beta} = 5.2\%$, $B_o = 4.8$ T, $C_u = 2359$ \$/kW, is a device very similar in size to MSR but with N_c increased (from 18 in the MSR design). Also, the coils in our model are wedge-shaped, to maximise the modulation, compared with box coils in MSR. The combination of wedge-shaped coils with an increase in N_c/p, which reduces the 'anti-helical' effect, should produce a transform closer to the design value than the MSR coil set. The unit cost, 2359 \$/kW$_e$, is higher than the estimate given by the MSR group [4]; 2150 \$/kW$_e$, and is also higher than the 'best-case' $p = 3$, $\ell = 2$ reactor described above, 2165 \$/kW$_e$.

6. CONCLUSIONS

The design and cost bases of a modular stellarator fusion reactor have been examined. It is shown that a configuration based on $\ell = 2$ symmetry is better able to support the beta required for economic electricity generation than $\ell \geq 3$. A small additional vertical field is required to improve the flux surface geometry at the highest beta. Physical scaling relationships are obtained which allow the parameters of a modular $\ell = 2$ stellarator to be defined with reasonable accuracy over a range of numbers of field periods, aspect ratios and sizes. The costs of such a reactor are estimated by scaling from the cost predictions for the Starfire tokamak reactor plant which, like the stellarator, is a continuously operating device.

The main results of this work are firstly that for minimum unit cost, a stellarator reactor should be of small aspect ratio, and secondly that it is possible to design such a system which is competitive in unit costs with the most optimistic tokamak reactor designs (eg Starfire). The best-case design, for a 4000 MWth plant, has a major radius of $\simeq$ 16 m, an average plasma minor radius of $\simeq$ 2 m, 3 field periods, a high transform per field period giving a total of $\simeq$ 0.5, 15 coils, a modest wall loading of 2 MW/m^2, a main field of 6.6 T and a modest average beta of 3.9%. The vacuum and equilibrium flux surfaces have been checked as far as possible using field-line following and analytic equilibrium calculations. The plant should produce $\simeq$ 1350 MW_e, which is higher than Starfire where 11% of the electrical power is recirculated to power the continuous current drive.

ACKNOWLEDGEMENTS

We should like to thank W.R. Spears, P.J. Fielding, P.R. Thomas, P.J. Lomas, D.J. Lees and R.J. Hastie for helpful discussions of various parts of this work and T.J. Martin for providing computer programs used for particle and field-line following calculations. One of us (WNGH) should like, in addition, to thank Merton College, Oxford, for a senior scholarship with the support of which this work was begun.

TABLE 1

		Unit	Value (Stellarator)	Value (Starfire)
1. Characteristic Machine Dimensions				
1.1	Reactor Envelope			
1.1.1	Height	m	15.8	28.6
1.1.2	Width	m	51 dia	33 dia
1.2	First Wall			
1.2.1	Major Radius	m	15.8	7
1.2.2	Minor Radius	m	2.17	2.14
1.2.3	Volume	m^3	1340	950
1.2.4	Inner Surface Area	m^2	1405	780
2. Plasma Parameters				
2.1	Plasma Dimensions			
2.1.1	Major Radius	m	15.8	7
2.1.2	Minor Radius	m	1.97 (1.38x2.56)	1.94
2.1.3	Elongation		1.86	1.6
2.8	Peak Toroidal Beta		0.058	0.194
2.18	q, Plasma Safety Factor		2.08	5.1
2.21	Plasma Heating Method		Lower Hybrid	
2.22	Plasma Heating Power	MW	160	90.4
3. Power Output				
3.2	Plasma Fusion Power	MWth	3510	
3.2.1	Thermal Power	MWth	4000	
3.3	Power to First Wall (neutron)	MWth	2810	
3.10	Plasma Chamber Power Density	MW/m^3	2.6	3.7
3.10.1	Plasma Power Density	MW/m^3	3.2	4.7
3.12	Plant Gross Electrical Output	MWe	1440	
3.13	Plant Net Electrical Output	MWe	1340	1200

		Unit	Value	Value
3.16	Net Plant Efficiency	%	33	30
9. Reactor Components				
9.1.8	First Wall Loading			
9.1.8.1	14.1 MeV neutrons (average)	MW/m^2	2.0	3.6
9.3.1	Toroidal Field Magnets			
9.3.1.8	Maximum Field	T	10.0	11.1
9.3.1.9	Field on Plasma Axis	T	6.6	5.8
9.3.1.10	Number of Magnets		15	12
9.3.2	Equilibrium Field Magnets			
9.3.2.9	Field on Axis	T	0.26	0.35
9.3.2.10	Number of Coils		2	6
11. Buildings				
11.1	Reactor Building			
11.1.1	Characteristic Dimensions			
	Reactor Hall	mxmxm	80x80x44	50x50x44
	Process Room	mxmxm	80x56x44	90x50x44
11.1.2	Enclosed Volume	m^3	$4.79\ 10^5$	$3.08\ 10^5$

TABLE 2

ACCOUNT NUMBER	ACCOUNT TITLE	COSTS (1980, $M)			
		TRELLA/ATOR		STARFIRE	
20	LAND AND LAND RIGHTS	3.3		3.30	
21	STRUCTURES AND SITE FACILITIES	450.1		346.58	
21.02	Reactor Buildings		261.6		157.44
22	REACTOR PLANT EQUIPMENT	1231.6		968.62	
22.01	Reactor Equipment		852.2		589.26
22.01.01	Blanket and First Wall		161.8		82.36
22.01.02	Shield		209.1		186.07
22.01.03	Magnets		308.1		171.57
22.01.04	R F Heating		58.7		33.49
22.01.07	Power Supply, Switching and Energy Storage		52.3		52.90
23	TURBINE PLANT EQUIPMENT	249.7		249.68	
24	ELECTRIC PLANT EQUIPMENT	117.3		117.28	
25	MISCELLANEOUS PLANT EQUIPMENT	40.8		40.77	
26	SPECIAL MATERIALS	0.3		0.25	
	TOTAL DIRECT COST	2093.1		1726.48	
91	CONSTRUCTION FACILITIES, EQUIPMENT AND SERVICES (10%)	209.3		172.65	
92	ENGINEERING AND CONSTRUCTION MANAGEMENT SERVICES (8%)	167.5		138.12	
93	OTHER COSTS (5%)	104.7		86.32	
	SUBTOTAL	2574.6		2123.57	
		1980 CONSTANT			
94	INTEREST DURING CONSTRUCTION (13%)	334.7		276.70	
95	ESCALATION DURING CONSTRUCTION (0%)	0.0		0.00	
	TOTAL CAPITAL	2908.3		2400.27	
	$/kW$_e$	2165		2000	

REFERENCES

[1] Shohet, J.L., "Ultimate and Modular Torsatrons", Proceedings of 2nd International Stellarator Workshop, Bavaria, F.R.G. (1980), paper B.3.4.

[2] Rehker, S. and Wobig, H., "Stellarator Fields with Twisted Coils", IPP 2/215 (1973).

[3] Sviatoslavsky, I., Van Sciver, S.W., Kulcinski, G.L., Anderson, D.T., Bailey, A.W., Callen, J.D., Derr, J.A., Emmert, G.A., El-Guebaly, L., Khalil, A., Shohet, J.L., Sze, D.K., Saunders, R.C. and Tataronis, J.A., IEEE Transactions on Plasma Science, PS-9 (1981) 163.

[4] Miller, R.L. and Krakowski, R.A., "The Modular Stellarator Fusion Reactor (MSR) Concept". 3rd IAEA Technical Committee Meeting and Workshop on Fusion Reactor Design and Technology, Tokyo, Japan (1981).

[5] Pfirsch, D., in Proceedings of the 5th Erice School on Fusion Reactor Technology, (to be published).

[6] Politzer, P.A., Lidsky, L.M. and Montgomery, D.B., "Torsatrons and the TOREX Proof-of-Principle Experiment", MIT report PFC/TR-79-1, (1979).

[7] Iiyoshi, I. and Uo, K., "Heliotron as a Steady Fusion Reactor", Proceedings of 5th International Conference on Plasma Physics and Controlled Nuclear Fusion Research, IAEA-CN-33/G4, III, 619, (1974).

[8] Carruthers, R., Davenport, P.A. and Mitchell, J.T.D., "The Economic Generation of Power from Thermonuclear Fusion", CLM-R85, (1967).

[9] Mitchell, J.T.D., "Blanket Replacement in Toroidal Fusion Reactors", 3rd ANS Topical Meeting on Technology of Controlled Nuclear Fusion, Sante Fe (1978), Invited Paper.

[10] Hitchon, W.N.G., Johnson, P.C. and Watson, C.J.H., "The Case for a Low Aspect Ratio, Modular Stellarator Reactor", in Proceedings 3rd International Stellarator Workshop, Moscow (1981).

[11] Baker, C.C., et al., "Starfire - a Commercial Tokamak Fusion Power Plant Study". AWL/FPP-80-1, (1980).

[12] Anderson, D.T., Derr, J.A. and Shohet, J.L., IEEE Transactions on Plasma Science, P5-9 (1981) 212.

[13] Chu, T.K., Furth, H.P., Johnson, J.L., Ludescher, C. and Weimer, K.E., Ibid, p 228.

[14] Hitchon, W.N.G. and Fielding. P.J., Nuclear Fusion, 21 (1981) 775.

[15] Gibson, A., Physics Fluids, 10 (1967) 1553.

[16] Fielding, P.J. and Hitchon, W.N.G., J. Plasma Physics, 24 (1980) 453.

[17] Lortz, D. and Nuhrenberg, J., Nuclear Fusion, 17 (1977) 125.

[18] Bernstein, I.B., Frieman, E.A., Kruskal, M.D. and Kulsrud, R.M., Proceedings Royal Society, A244, (1958) 17.

[19] Shohet, J.L. and Anderson, D.T., Comments on Plasma Physics and Controlled Fusion, 7 (1982) 103.

[20] Shafranov, V.D. and Yurchenko, E.I., Soviet Physics, JETP, 26 (1968) 682.

[21] Glasser, A.H., Greene, J.M. and Johnson, J.L., Physics Fluids, 18 (1975) 87.

[22] Mikhailovskii, A.B., Nuclear Fusion, 15 (1975) 95.

[23] Spears, W.R. and Wesson, J.A., Nuclear Fusion, 20 (1980) 1525.

[24] WVII-A Team, Plasma Physics and Controlled Nuclear Fusion Research, (1978) paper IAEA-CN-37/H-2.

[25] Derr, J.A. and Shohet, J.L., IEEE transactions on Plasma Science, PS-9 (1981) 234.

[26] Karger, F. and Lackner, K., Phys. Lett., 61A (1977) 385.

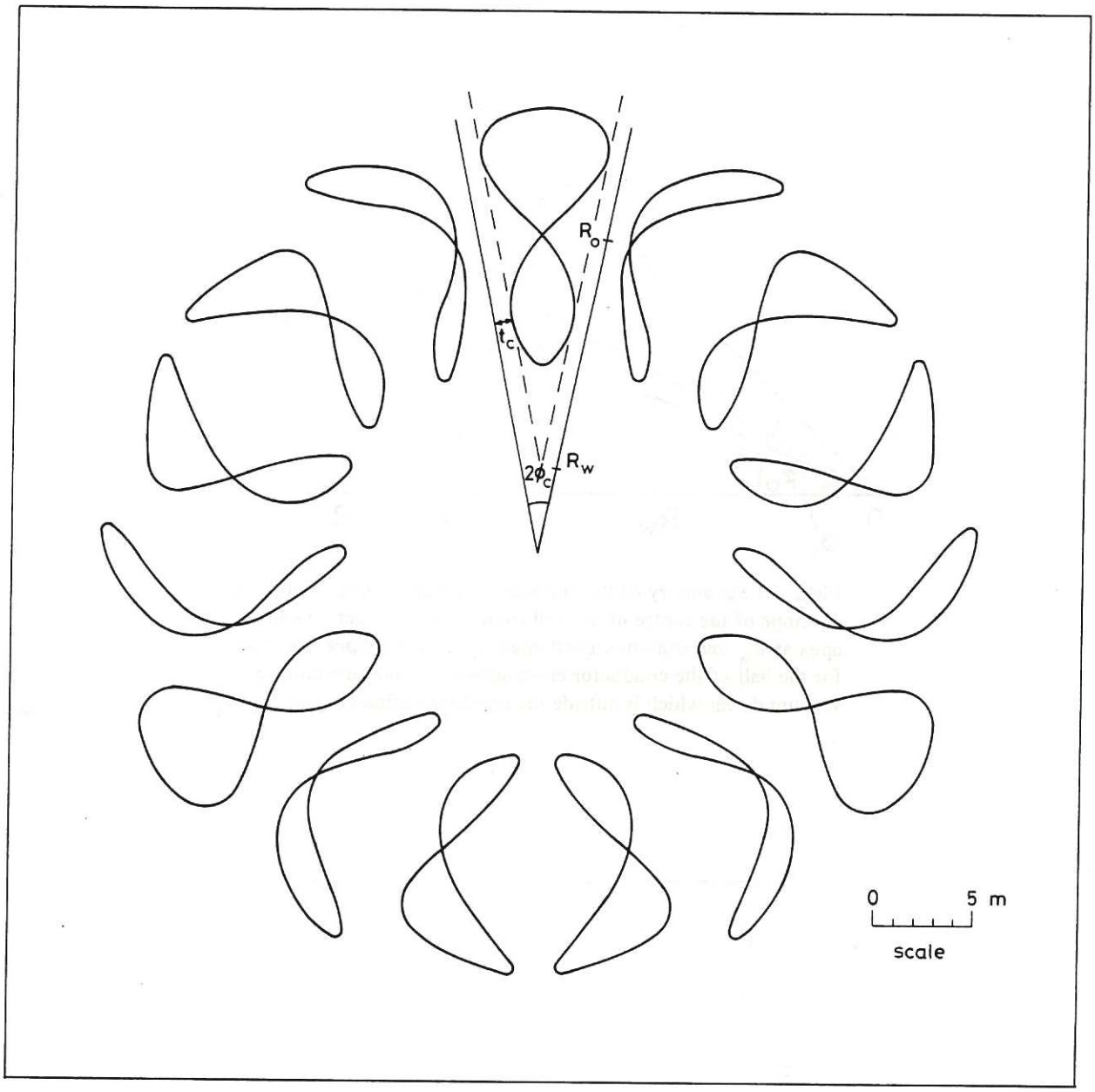

Fig.1 A 15 coil, 3 field period, $\ell = 2$ modular stellarator with wedge shaped coils, represented as filaments, and a coil aspect ratio $\simeq 3$.

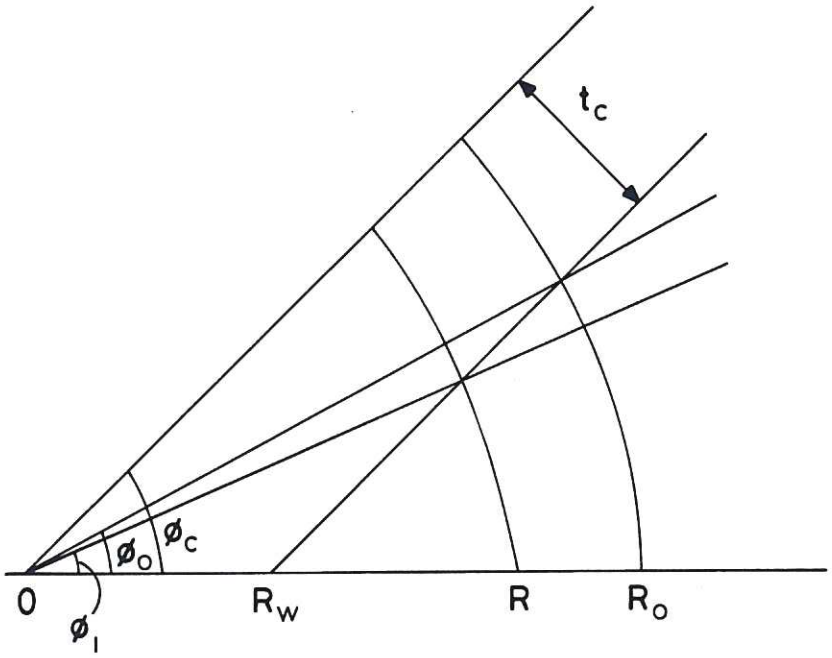

Fig.2 The geometry of the envelope of a wedge shaped coil. The envelope of the centre of the coil conductor cross-section has its apex at R_W and subtends a half-angle ϕ_c. t_c is the space allowed for the half of the conductor cross-section and the surrounding vacuum dewar which is outside the envelope defined by R_W and ϕ_c.

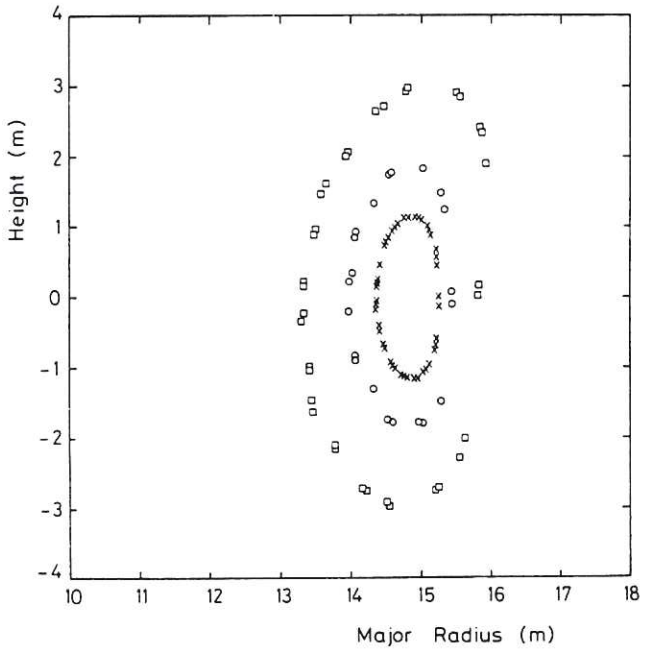

Fig.3 Vacuum magnetic surfaces, computed by field line following, for the coil set in Figure 1.

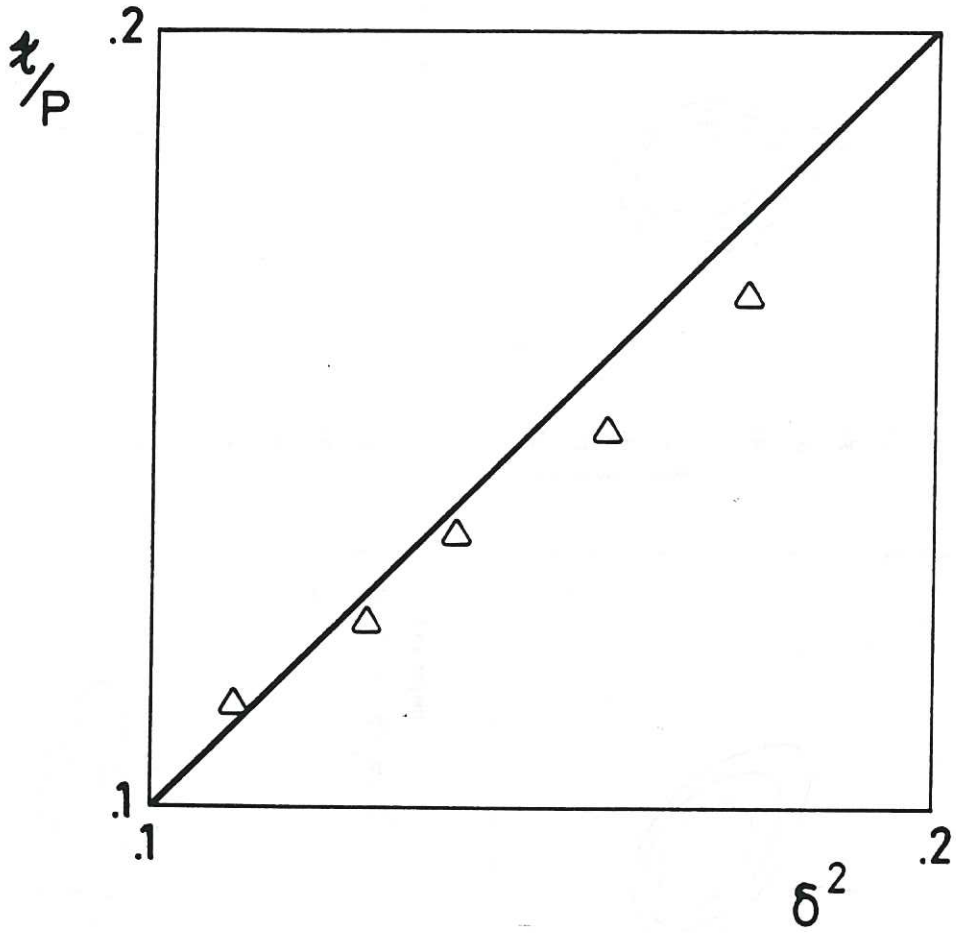

Fig.4 The variation of transform per field period t/p with δ^2, computed by field line following. The solid line is the theoretical prediction $t/p = \delta^2$.

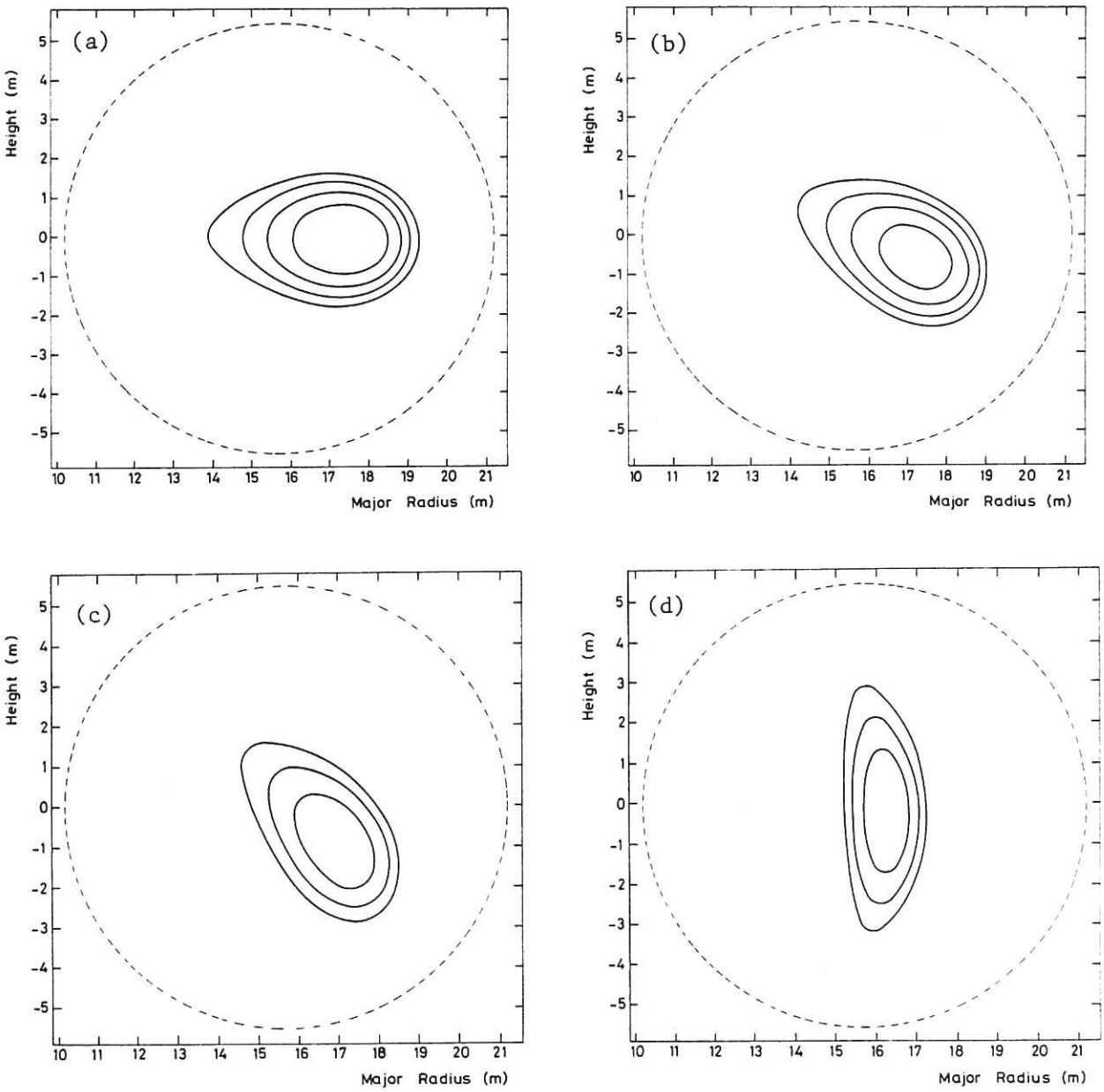

Fig.5 Computed equilibrium magnetic surfaces for an $\ell = 2$ stellarator with $p = 3$, $\tau = 0.48$ and $A_p = 8$, at an average beta of $\bar{\beta} = 3.9\%$ for a quartic pressure profile and with a vertical field $B_v = 0.04B_o$. Four sections within a field period are shown. The dashed line is the mean coil radius.

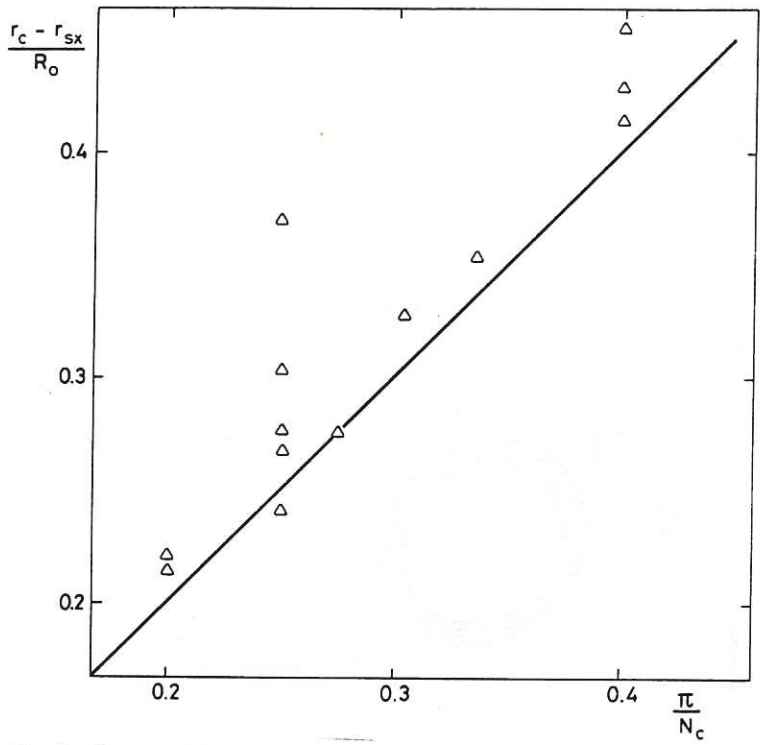

Fig.6 The position of the separatrix in a modular $\ell = 2$ stellarator. The distance of the separatrix inside the coil $r_c - r_{sx}$, normalised to the coil major radius R_o, is shown against π/N_c. In some cases, resonant errors in the field have decreased r_{sx}, but in the absence of field errors the computed points are close to the line $(r_c - r_{sx})/R_o = \pi/N_c$.

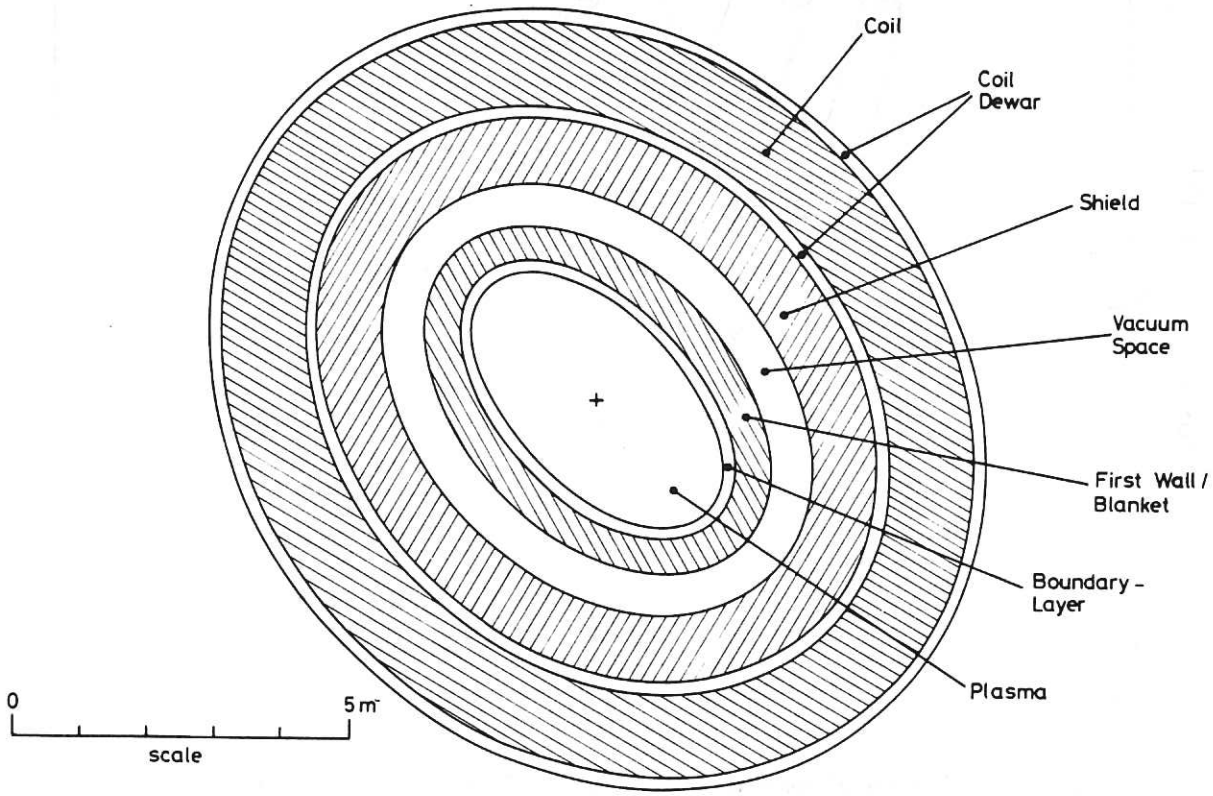

Fig.7 A schematic view of the cross section through a module of a stellarator reactor based on Starfire engineering concepts.

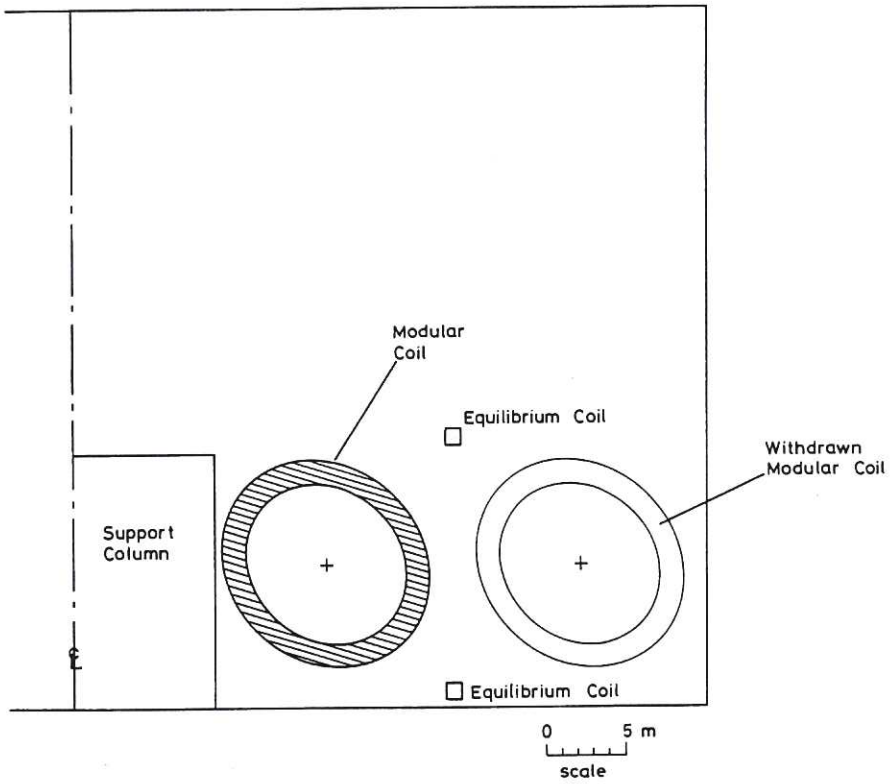

Fig.8 A schematic view of the cross-section through the reactor hall showing a coil module in position and withdrawn. The positions of the vertical field coils are also shown.

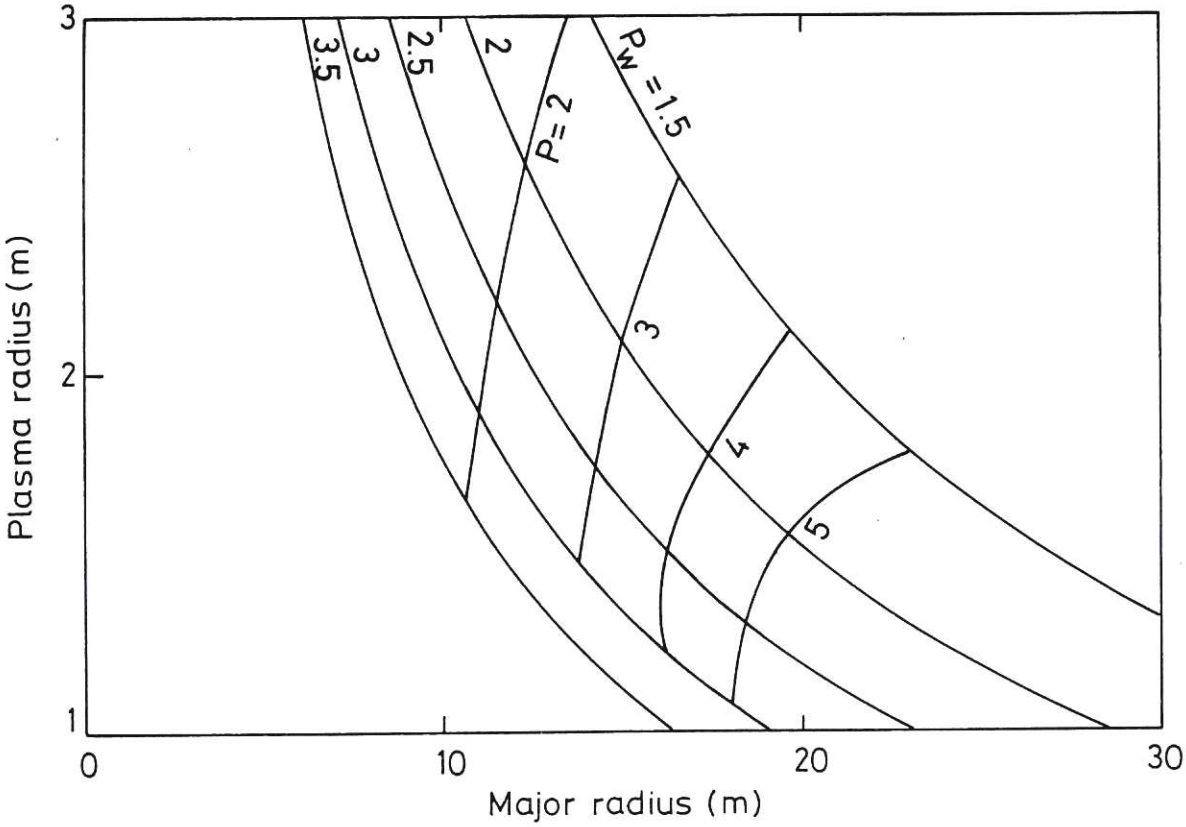

Fig.9 The variation of plasma minor radius r_p with major radius R_o for fixed values of p, the number of field periods, and P_w, the neutron wall loading. Only devices with the minimum permissible R_o at given p and P_w are shown.

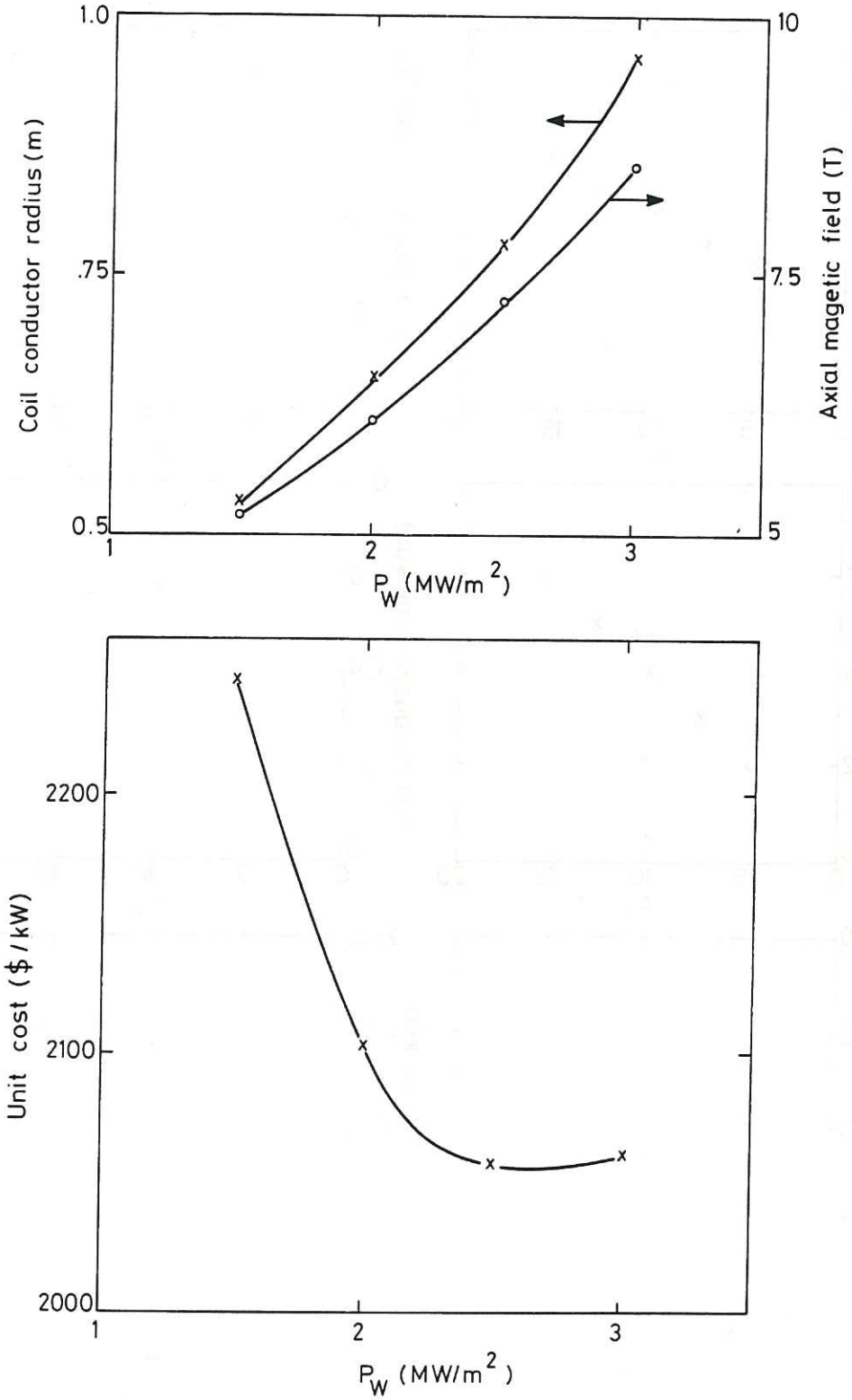

Fig.10 The variation of parameters and costs with wall loading, P_w, for 3 field period stellarator reactors. (a) The magnetic field on axis and the radius of the coil conductor cross-section; (b) the unit cost ($/kW).

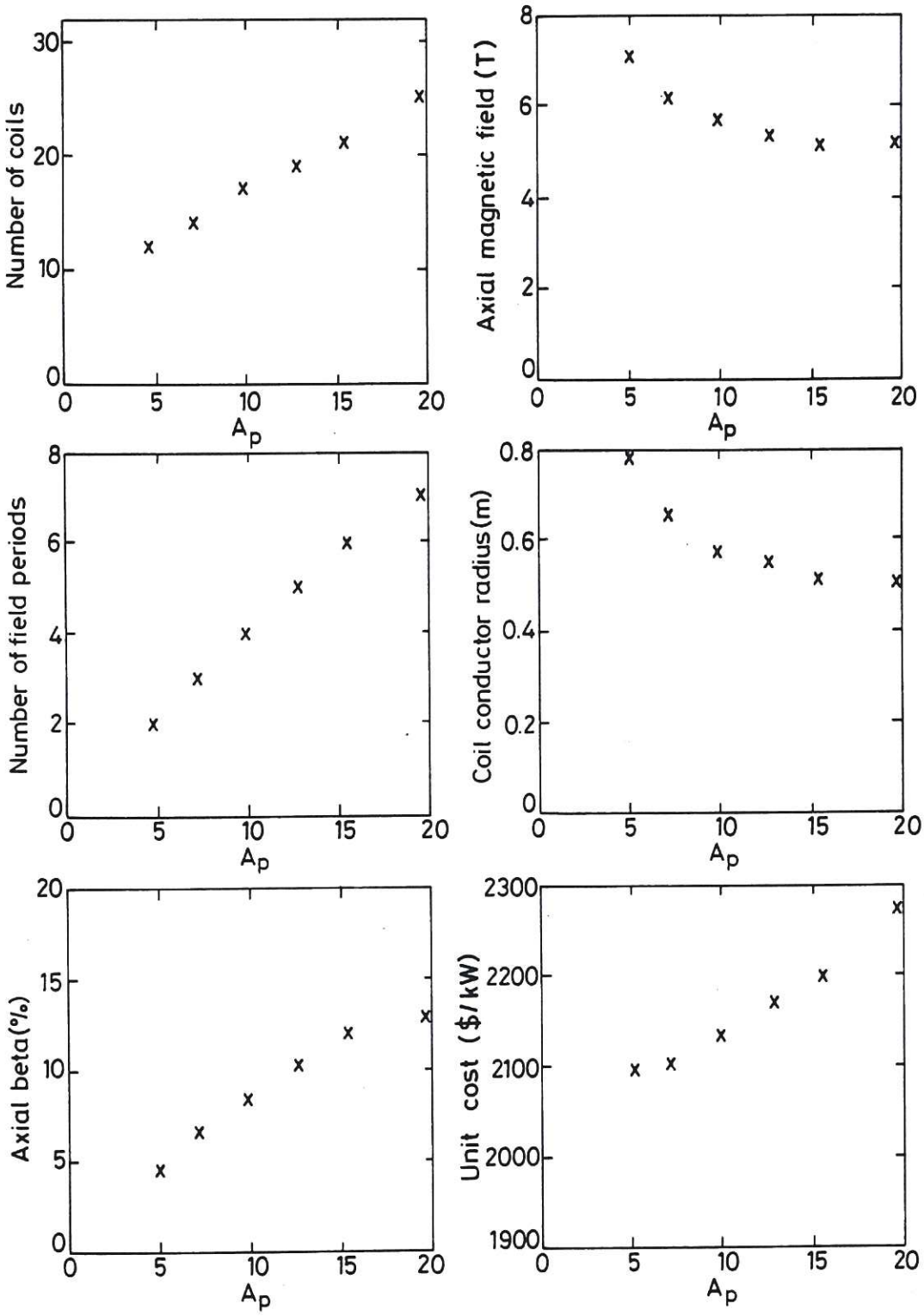

Fig.11 The variation with plasma aspect ratio of the main parameters of a stellarator reactor for a wall loading $P_w = 2 MW/m^2$.

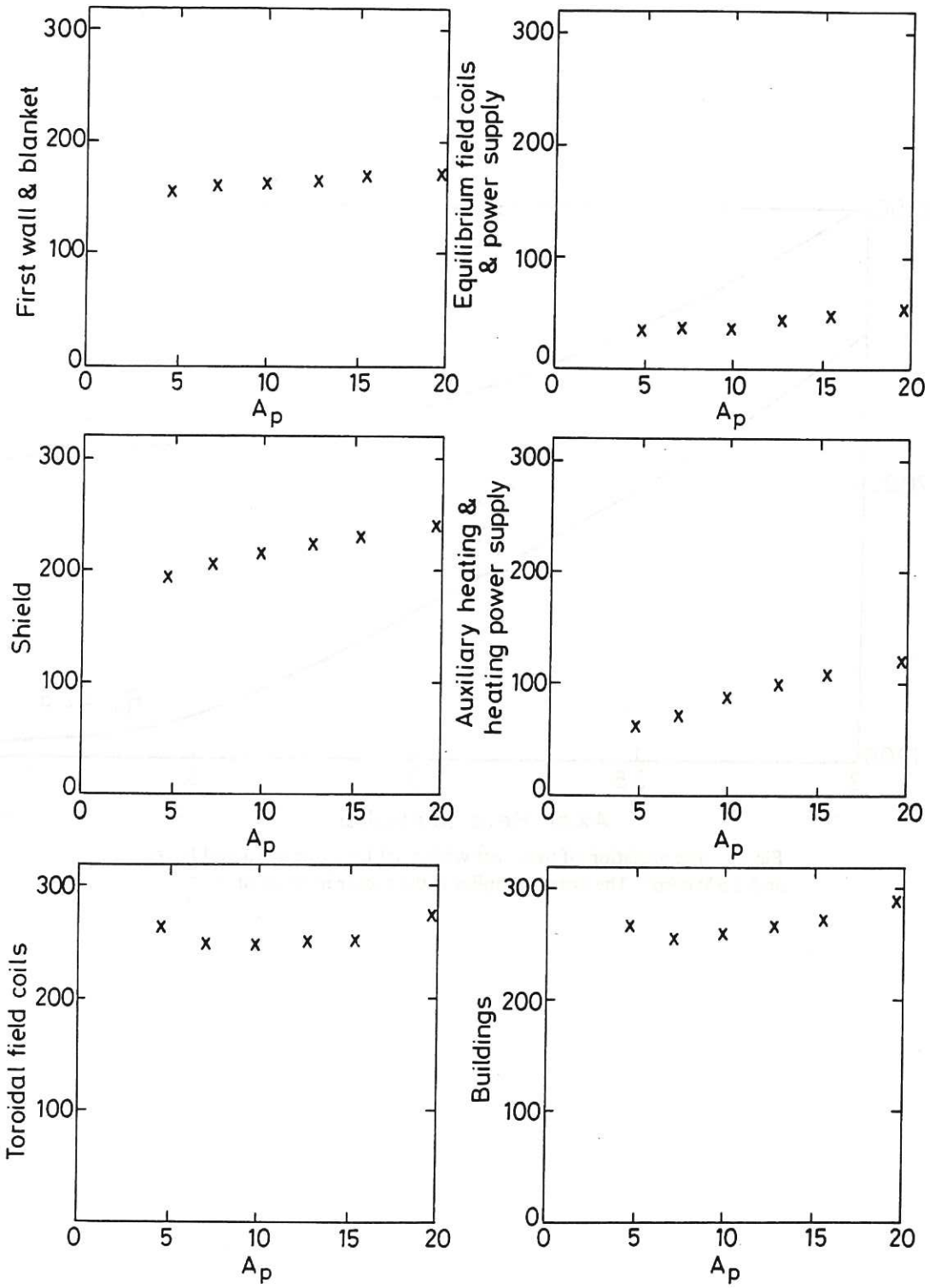

Fig.12 The variation in cost of the major components of a stellarator reactor with plasma aspect ratio for a wall loading of $P_w = 2 MW/m^2$.

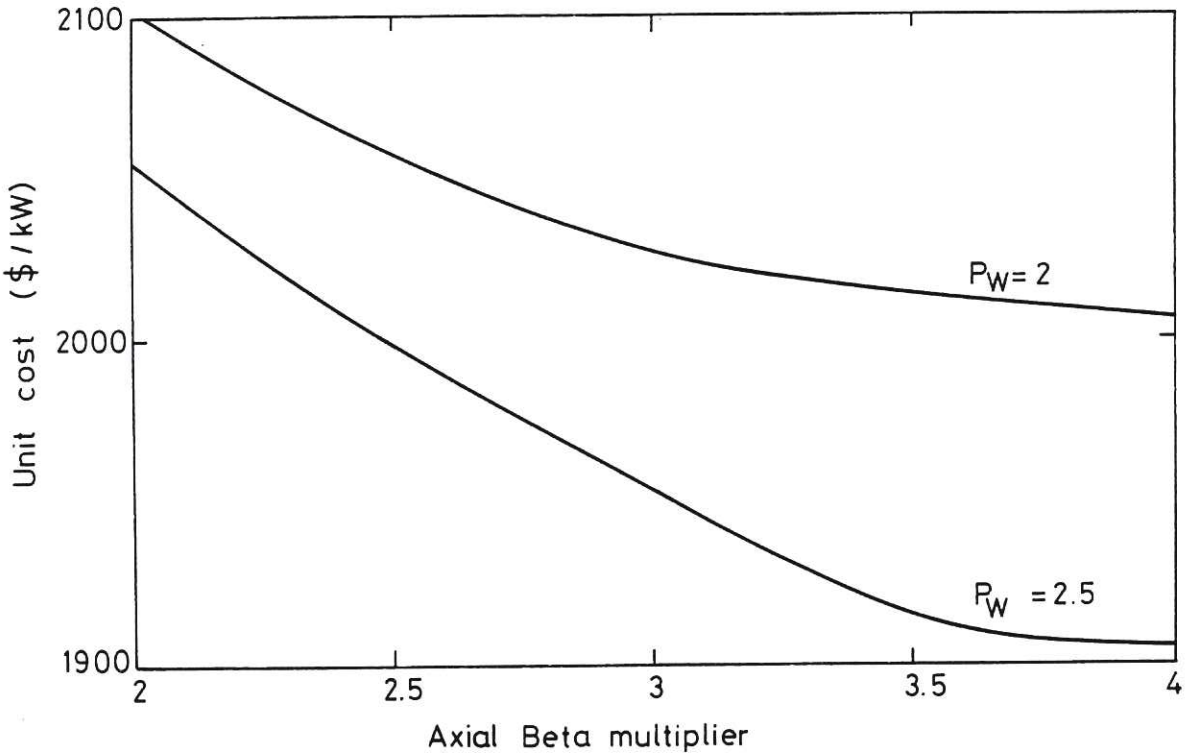

Fig.13 The variation of unit cost with axial beta, for p = 3 and P_w = 2 and 2.5 MW/m^2. The beta multiplier is the factor in front of $\tau^2 \epsilon_p$.